
UniOD: A Universal Model for Outlier Detection across Diverse Domains

Dazhi Fu Jicong Fan*

School of Data Science

The Chinese University of Hong Kong, Shenzhen, China

Abstract

Outlier detection (OD) seeks to distinguish inliers and outliers in completely unlabeled datasets and plays a vital role in science and engineering. Most existing OD methods require troublesome dataset-specific hyperparameter tuning and costly model training before they can be deployed to identify outliers. In this work, we propose UniOD, a universal OD framework that leverages labeled datasets to train a single model capable of detecting outliers of datasets from diverse domains. Specifically, UniOD converts each dataset into multiple graphs, produces consistent node features, and frames outlier detection as a node-classification task, and is able to generalize to unseen domains. As a result, UniOD avoids effort on model selection and hyperparameter tuning, reduces computational cost, and effectively utilizes the knowledge from historical datasets, which improves the convenience and accuracy in real applications. We evaluate UniOD on 15 benchmark OD datasets against 15 state-of-the-art baselines, demonstrating its effectiveness.

1 Introduction

Outliers are observations that deviate substantially from other normal data in a dataset, indicating they likely arise from a distinct generative process. In data-driven applications, detecting and removing outliers is vital, since their presence can severely degrade the accuracy and robustness of downstream analyses. The problem of identifying such anomalies—commonly termed outlier detection (OD) [Hodge and Austin, 2004; Chandola *et al.*, 2009; Ruff *et al.*, 2021], anomaly detection [Pang *et al.*, 2021], or novelty detection [Pimentel *et al.*, 2014]—has attracted extensive research. OD techniques serve a variety of purposes [Singh and Upadhyaya, 2012; Ahmed *et al.*, 2016; Breier and Branišová, 2017], including preprocessing for supervised learning to eliminate aberrant samples, healthcare diagnostics and monitoring, fraud detection in financial transactions and cybersecurity, and beyond.

In the past few decades, many OD methods have been proposed. Basically, we can divide them into two categories: traditional methods and deep-learning (neural network) based methods. Traditional methods often use kernel methods, nearest-neighbor distance, decision trees and other techniques to build their model. For instance, kernel density estimation (KDE) [Parzen, 1962] uses kernel function to estimate density of each data as its outlier score, k NN [Ramaswamy *et al.*, 2000] uses the distance from an observation to its k nearest neighbors as its outlier score, local outlier factor (LOF) [Breunig *et al.*, 2000a] compares the local density of an observation to the local densities of its neighbors and identify observations that have a substantially lower density than their neighbors as outliers. Isolation Forest [Liu *et al.*, 2008] assumes that outliers are more susceptible to isolation than normal observations and uses random decision trees recursively to partition the feature space, where outliers tend to be separated into leaf nodes in far fewer splits. As for deep learning based methods, these methods use neural networks for feature extraction, dimensionality reduction, or other purposes. For instance, DeepSVDD [Ruff *et al.*, 2018a] uses a neural network to project samples into a hypersphere

*Corresponding author

and uses the distance to the center of hypersphere as outlier score, NeutralAD [Qiu *et al.*, 2021] uses augmentations on data and map the augmented data and original data into a space where the embedding of augmented data remains similar to that of the original data, DTE [Livernoche *et al.*, 2023a] simplifies DDPM by estimating the distribution over diffusion time for a given input and uses the mode or mean of this distribution as the outlier score instead of reconstruction distance. In ODIM [Kim *et al.*, 2024], authors observe the memorization effect and train several under-fitted generative models and use the average reconstruction error over these models as an outlier score.

The OD methods mentioned above, especially those based on deep learning, are dataset-specific as shown in Figure 1. That means, for a new dataset, especially when it is from a different domain, we have to train an OD model from scratch, which has the following limitations:

- **High effort on model selection and hyperparameter tuning** Particularly, for deep learning based OD methods, we need to determine the network depth, width, learning rate, and method-specific hyperparameters.
- **High computational cost and waiting time before deployment** The training is often time-consuming, especially when the model size and data size are both large.
- **Waste of knowledge from historical datasets** Historical datasets often contain useful and transferable knowledge about inlier and outlier patterns, which cannot be used by the conventional OD methods.

In this work, we aim to address the three limitations above by constructing a universal outlier detection model, called UniOD. The main idea is to use historical labeled datasets to train a universal model capable of detecting outliers for all other tabular datasets without retraining. Specifically, we build a kernel-based similarity graph for each historical dataset, then apply decomposition to its adjacency matrix to extract uniformly dimensioned node embeddings, thus harmonizing disparate original feature dimensions. We then train a graph neural network (GNN) on these graphs generated by historical datasets to perform node classification, distinguishing inliers from outliers. After training, for any newly unseen tabular datasets, UniOD converts it into a similarity graph using the same kernel-decomposition pipeline and applies the pretrained GNN to identify outliers inside it. An overview of UniOD is shown in Figure 2. Our contributions are as follows.

- We propose a novel method for outlier detection called UniOD. UniOD is able to leverage knowledge from historical datasets and directly classify outliers inside a newly unseen dataset without training.
- UniOD has much lower model complexity compared to other deep learning based methods since outlier detection on all datasets can be done using one single model. Additionally, UniOD has a lower time complexity for outlier detection since the training procedure is skipped.
- We conduct experiments on 15 datasets and compare UniOD against 15 baseline methods, where UniOD outperforms most of them.

2 Related Work

2.1 OD Methods without Model Training

In outlier detection, several widely-used nonparametric methods obviate the need for an explicit training phase. The method k nearest neighbor (kNN) [Ramaswamy *et al.*, 2000] computes each sample’s outlier score as the average distance to its k nearest neighbors. Kernel density estimation (KDE) [Parzen, 1962] employs kernel functions to estimate the underlying probability density, treating points with low estimated density as outliers. The local outlier factor (LOF) [Breunig *et al.*, 2000a] defines a reachability distance based on k NN distances to estimate each point’s local density and then compares it to the densities of its neighbors—points whose local density is substantially lower than that of their neighbors receive higher outlier scores. In ECOD [Li *et al.*, 2022a], the authors observe that outliers are often rare events in the tails of a distribution. Then the algorithm first estimates, for each feature dimension, the empirical cumulative distribution function of the input data; it then uses these marginal ECDFs to compute one-sided tail probabilities for every data point in each dimension; finally, it aggregates these per-dimension tail-probability estimates—typically by summation—to

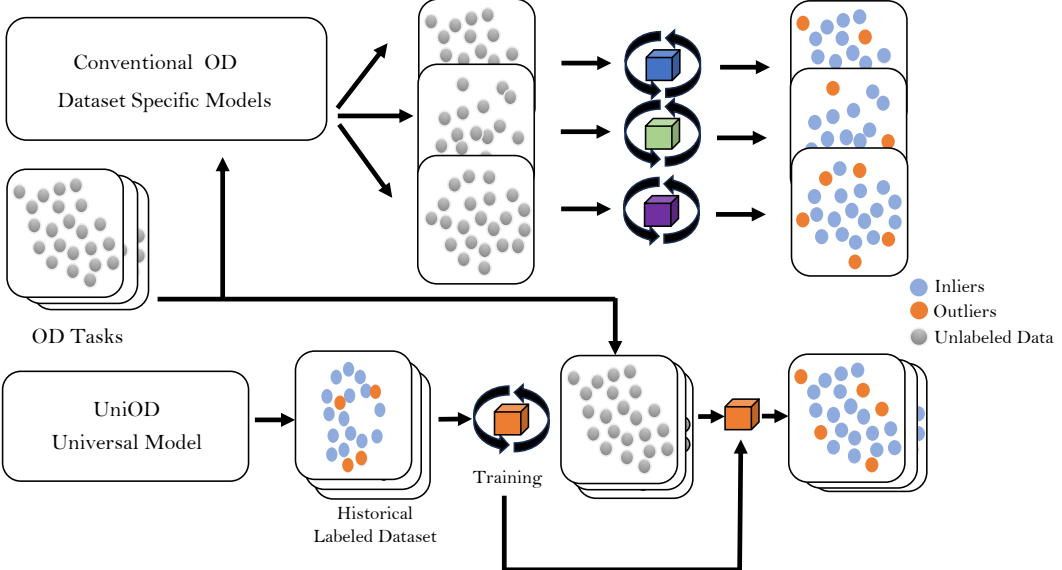


Figure 1: Pipeline of UniOD and conventional OD methods. These approaches use a separate model on each dataset for outlier detection. In contrast, UniOD leverages a collection of historical labeled datasets to train a single universal model, which is capable of detecting outliers in different datasets.

produce a single outlier score, thereby highlighting samples that are anomalously extreme along one or more feature axes.

2.2 Hyperparameter Optimization and Model Selection for OD

Previous studies [Goldstein and Uchida, 2016; Ding *et al.*, 2022] have shown that OD methods can be sensitive to hyperparameter changes. In the past few years, many methods have been proposed to solve the problem and to select the best hyperparameters for OD models. MetaOD [Zhao *et al.*, 2020] capitalizes on the past performances of a large body of detection models on existing outlier detection benchmark datasets, and uses collaborative filtering to automatically select effective hyperparameters to be employed on a new dataset without using any labels. ROBOD [Ding *et al.*, 2022] combines scores from a collection of models and remedies the “choice paralysis” by assembling various autoencoder models of different hyperparameter configurations, hence obviating hyperparameter selection. ELECT [Zhao *et al.*, 2022] uses prior knowledge like model performance from historical datasets and uses similarity between datasets for hyperparameter selection. HPOD [Zhao and Akoglu, 2022] capitalizes on the prior performance of a large collection of hyperparameters on existing OD benchmark datasets and uses a regressor to fit hyperparameters and their performance. PyOD2 [Chen *et al.*, 2024b] uses a large language model (LLM) to analyze the properties of each OD model and dataset, then uses these models and dataset tags, combined with LLM-based reasoning, to identify the most suitable model. MetaOOD [Qin *et al.*, 2024] uses language models to generate embeddings for data and collaborative filtering to fit a performance matrix on historical datasets and select the most effective method for a new out-of-distribution (OOD) task. Although hyperparameter optimization methods can improve the performance of OD models in many datasets, they exhibit important limitations: they require exhaustive training and evaluation over all candidate hyperparameter combinations on historical datasets, incurring substantial computational and time costs—a burden that grows even heavier when applied to deep learning based OD models. Note that Dai and Fan [2025] proposed a method for model and hyperparameter selection in anomaly detection (inductive learning), which does not apply to outlier detection (transductive learning).

2.3 Transfer Learning for OD

Transfer learning [Van Haaren *et al.*, 2015; Weiss *et al.*, 2016] is a machine-learning paradigm in which a model trained on one problem (the source task and its data) is repurposed to solve a different, but related, problem (the target task and its data). Since acquiring large quantities of labeled data for specific OD tasks can be expensive or infeasible, and different OD tasks may exhibit shared structure

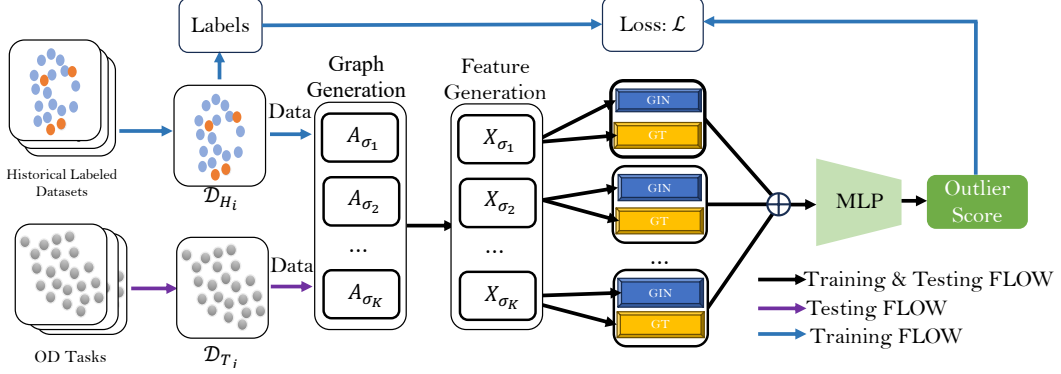


Figure 2: Framework of our proposed UniOD. UniOD leverages a collection of historical labeled datasets to train a single, universal GNN-based classifier capable of detecting outliers for datasets with different data dimensions across diverse domains.

or property, there have been several works exploring the use of transfer learning for outlier and anomaly detection [Andrews *et al.*, 2016; Vercruyssen *et al.*, 2017; Vincent *et al.*, 2020]. In [Andrews *et al.*, 2016], the authors proposed two transfer learning frameworks for anomaly detection on image data: transfer learning of pre-trained deep convolutional representations and transfer learning of deep convolutional representations from an auxiliary task. In [Vincent *et al.*, 2020], the proposed LOCIT selects and transfers relevant labeled instances from a source OD task to a target one. Then, it classifies target instances using the nearest-neighbors technique that considers both unlabeled target and transferred labeled source instances. Although these transfer methods are prone to being useful and effective in many datasets, they share critical limitations. First, transfer learning requires the source datasets to be closely related to the target domain requirement that is often unmet in practice, particularly for heterogeneous tabular data. Moreover, these methods all require source and target data to have the same-dimensional features with the same semantics, effectively excluding the use of source datasets with different dimensions or different semantics.

3 Methodology

3.1 Problem Statement

Formally, let T_i denote “task i ”, and let $\mathcal{D}_{T_i} = \{\mathbf{x}_{T_i}^{(1)}, \mathbf{x}_{T_i}^{(2)}, \dots, \mathbf{x}_{T_i}^{(n_{T_i})}\}$ be a set of d_{T_i} -dimensional data and assume that it can be partitioned into two subsets, $\mathcal{D}_{T_i}^{\text{inlier}}$ and $\mathcal{D}_{T_i}^{\text{outlier}}$, where $|\mathcal{D}_{T_i}^{\text{inlier}}| \gg |\mathcal{D}_{T_i}^{\text{outlier}}|$ and the data points in $\mathcal{D}_{T_i}^{\text{inlier}}$ are drawn from an unknown distribution with a density function p_{inlier} such that $p_{\text{inlier}}(\mathbf{x}) > p_{\text{inlier}}(\mathbf{x}')$ holds for any $\mathbf{x} \in \mathcal{D}_{T_i}^{\text{inlier}}$ and $\mathbf{x}' \in \mathcal{D}_{T_i}^{\text{outlier}}$. The primary task of outlier detection (OD) is to identify $\mathcal{D}_{T_i}^{\text{outlier}}$ from \mathcal{D}_{T_i} .

Notably, suppose there are B datasets, $\mathcal{D}_{T_1}, \mathcal{D}_{T_2}, \dots, \mathcal{D}_{T_B}$, from B different domains, corresponding to B independent OD tasks, existing OD methods train one model on each dataset independently, which implies B times of hyperparameter tuning and model training. In addition, the knowledge from datasets across different domains is overlooked. For a new dataset $\mathcal{D}_{T_{B+1}}$, we need to train an OD model from scratch.

3.2 Proposed Method

To tackle the challenges faced by previously proposed OD methods, we propose UniOD, which is able to use labeled historical datasets, easily available in this big data era, to train a general model that can detect outliers in a dataset from any unseen domain without conducting any retraining. Specifically, let $\mathcal{D}_H = \{\mathcal{D}_{H_1}, \mathcal{D}_{H_2}, \dots, \mathcal{D}_{H_M}\}$ be a set of M historical labeled datasets, which means:

$$\begin{aligned} \forall i \in \{1, 2, \dots, M\}, \mathcal{D}_{H_i} &= \{(\mathbf{x}_{H_i}^{(1)}, \mathbf{y}_{H_i}^{(1)}), (\mathbf{x}_{H_i}^{(2)}, \mathbf{y}_{H_i}^{(2)}), \dots, (\mathbf{x}_{H_i}^{(n_{H_i})}, \mathbf{y}_{H_i}^{(n_{H_i})})\} \\ \forall j \in \{1, 2, \dots, n_{H_i}\}, \mathbf{x}_{H_i}^{(j)} &\in \mathbb{R}^{d_{H_i}}, \mathbf{y}_{H_i}^{(j)} \in \{(0, 1), (1, 0)\} \end{aligned} \quad (1)$$

where n_{H_i} and d_{H_i} denotes the number and dimension of data in historical dataset \mathcal{D}_{H_i} respectively. $\mathbf{y}_{H_i}^{(j)} = (0, 1)$ indicates that the sample is an outlier. Also, let $\mathcal{D}_T = \{\mathcal{D}_{T_1}, \mathcal{D}_{T_2}, \dots, \mathcal{D}_{T_B}\}$ be a set of B unlabeled test datasets. The primary goal of UniOD is to train a universal deep-learning based model based on these historical datasets \mathcal{D}_H , which can directly detect outliers in these test datasets \mathcal{D}_T without any further training or tuning.

3.2.1 Graph-based Data Unification of UniOD

Considering that datasets often differ in dimensionality, feature semantics, and sample size, we first apply preprocessing to harmonize their feature spaces—standardizing both the number of dimensions and the semantic interpretation of each feature. Our key idea is to represent the datasets as graphs, since a well-designed graph can capture the local and global structures of a dataset, and graph-based methods, such as spectral clustering, provide promising performance in solving various machine learning problems. Specifically, for each dataset \mathcal{D}_{H_i} , we calculate an adjacency matrix $A_{H_i, \sigma}$, which induces a weighted graph, using a Gaussian kernel function with hyperparameter σ , i.e.,

$$\forall a, b \in \{1, 2, \dots, n_{H_i}\}, \mathbf{A}_{H_i, \sigma}^{(a, b)} = \exp\left(\frac{-\|\mathbf{x}_{H_i}^{(a)} - \mathbf{x}_{H_i}^{(b)}\|^2}{2\sigma^2}\right) \quad (2)$$

Here, we encounter two problems. The first one is how to select an appropriate σ for (2). The other is that converting a whole dataset into one single graph will result in too much loss of information. To solve the two problems, we choose K different σ , denoted as $\sigma_1, \sigma_2, \dots, \sigma_K$, and each is determined by $\sigma_k = \beta_k \bar{\sigma}$, where β_k takes a value around 1 and $\bar{\sigma}$ is set as the average distance between the data points in \mathcal{D}_{H_i} , i.e., $\bar{\sigma} = \frac{1}{n_{H_i}^2} \sum_{\mathbf{x} \in \mathcal{D}_{H_i}} \sum_{\hat{\mathbf{x}} \in \mathcal{D}_{H_i}} \|\mathbf{x} - \hat{\mathbf{x}}\|$. Consequently, we generate multiple graphs for each dataset, with adjacency matrices $\mathcal{A}_{H_i} = \{\mathbf{A}_{H_i, \sigma_k}\}_{k=1}^K$. For each graph $\mathbf{A}_{H_i, \sigma_k}$, we use singular value decomposition (SVD) to generate uniformly dimensioned node features for different datasets:

$$\begin{aligned} \mathbf{A}_{H_i, \sigma_k} &= [\mathbf{u}_1, \mathbf{u}_2, \dots, \mathbf{u}_{n_{H_i}}] \text{diag}(\lambda_1, \lambda_2, \dots, \lambda_{n_{H_i}}) [\mathbf{v}_1, \mathbf{v}_2, \dots, \mathbf{v}_{n_{H_i}}]^\top \\ \mathbf{X}_{H_i, \sigma_k} &= [\mathbf{u}_1, \mathbf{u}_2, \dots, \mathbf{u}_{d^*}] \text{diag}(\lambda_1^{1/2}, \lambda_2^{1/2}, \dots, \lambda_{d^*}^{1/2}) \end{aligned} \quad (3)$$

where $0 < d^* < n_{H_i}$ is the unified feature dimension. For convenience, we write $\mathbf{X}_{H_i, \sigma_k} = [\tilde{\mathbf{x}}_{H_i, \sigma_k}^{(1)}, \tilde{\mathbf{x}}_{H_i, \sigma_k}^{(2)}, \dots, \tilde{\mathbf{x}}_{H_i, \sigma_k}^{(n_{H_i})}]^\top \in \mathbb{R}^{n_{H_i} \times d^*}$ is the uniformly dimensioned node feature matrix of graph k , $k = 1, 2, \dots, K$. As a result, for the whole $\mathcal{D}_H = \{\mathcal{D}_{H_1}, \mathcal{D}_{H_2}, \dots, \mathcal{D}_{H_M}\}$, we obtain

$$\mathcal{X}_H = \{\tilde{\mathbf{X}}_{H_1}, \tilde{\mathbf{X}}_{H_2}, \dots, \tilde{\mathbf{X}}_{H_M}\} \quad (4)$$

where $\tilde{\mathbf{X}}_{H_i} = (\mathbf{X}_{H_i, \sigma_1}, \dots, \mathbf{X}_{H_i, \sigma_K}) \in \mathbb{R}^{n_{H_i} \times Kd^*}$. Similarly, for the whole $\mathcal{D}_T = \{\mathcal{D}_{T_1}, \mathcal{D}_{T_2}, \dots, \mathcal{D}_{T_B}\}$, we have

$$\mathcal{X}_T = \{\tilde{\mathbf{X}}_{T_1}, \tilde{\mathbf{X}}_{T_2}, \dots, \tilde{\mathbf{X}}_{T_B}\} \quad (5)$$

The role of converting every dataset into multiple graphs and extracting SVD-based features is explained as follows:

- Graph construction combined with SVD embedding removes dependence on original feature dimensionality and semantics, enabling a unified representation across heterogeneous datasets.
- The adjacency matrix $\mathbf{A}_{H_i, \sigma_k}$ encodes pairwise affinities between samples, providing a deterministic, data-driven signal that informs outlier scoring.
- By modeling each dataset as graphs, we can utilize graph neural networks, to be introduced later, that propagate information through local neighborhoods, capturing how a node's relationship to its neighbors correlates with its anomalousness.
- By applying a simple subsampling technique to each historical dataset, to be introduced later, we can generate a diverse collection of graph-structured data for training UniOD, which will substantially enhance its generalization capability.

3.2.2 Model Design of UniOD

After generating graph-structured data and its uniformly dimensioned features, we can convert the OD task in these historical datasets \mathcal{D}_H as node classification tasks for each graph. Here, we use an K L_1 -layer graph isomorphism network (GIN) [Xu *et al.*, 2018] and an K L_2 -layer graph transformer (GT) to build our model, since each $\tilde{\mathbf{X}}_{H_i}$ is composed of K blocks. Specifically, we let

$$\mathbf{Z}_{H_i}^{\text{GIN}} = \text{KGIN}_{\theta_1} \left(\tilde{\mathbf{X}}_{H_i}, \mathcal{A}_{H_i} \right), \quad i = 1, \dots, M \quad (6)$$

$$\mathbf{Z}_{H_i}^{\text{GT}} = \text{KGT}_{\theta_2} \left(\tilde{\mathbf{X}}_{H_i} \right), \quad i = 1, \dots, M \quad (7)$$

where θ_1 and θ_2 denote the parameters of the GINs and GTs, respectively. The details are provided in *Appendix A*. Then the final embedding is the following concatenation

$$\mathbf{Z}_{H_i} = [\mathbf{Z}_{H_i}^{\text{GIN}}, \mathbf{Z}_{H_i}^{\text{GT}}] \in \mathbb{R}^{n_{H_i} \times \hat{d}} \quad (8)$$

where \hat{d} is the dimension of final embedding. Then we apply a L_3 -layer MLP with parameters θ_3 followed by a softmax function to predict the labels:

$$\hat{\mathbf{Y}}_{H_i} = \text{softmax} (\text{MLP}_{\theta_3} (\mathbf{Z}_{H_i})), \quad i = 1, \dots, M \quad (9)$$

where $\text{MLP}_{\theta_3} : \mathbb{R}^{\hat{d}} \rightarrow \mathbb{R}^2$. Then, we minimize cross entropy loss $\mathcal{L}(\theta)$ to train our proposed UniOD:

$$\mathcal{L}(\theta) = -\frac{1}{M} \sum_{i=1}^M \sum_{j=1}^{n_{H_i}} \left\langle \mathbf{y}_{H_i}^{(j)}, \log \hat{\mathbf{y}}_{H_i}^{(j)} \right\rangle \quad (10)$$

where $\theta = \{\theta_1, \theta_2, \theta_3\}$ denote all parameters of our model. After training, we obtain the trained parameters θ^* . For each specific testing dataset $\mathcal{D}_{T_i} \in \mathcal{D}_T$, we can use (2) and (3) to construct multiple graph-structured data and obtain $\tilde{\mathbf{X}}_{T_i}, \mathcal{A}_{T_i}$, and then we can input these graphs into our trained GINs and GTs to obtain \mathbf{Z}_{T_i} , and finally use the trained classifier $\text{MLP}_{\theta_3^*}$ to obtain the outlier score for each data point:

$$\text{Outlier Score}(\mathbf{x}_{T_i}^{(j)}) = [\hat{\mathbf{y}}_{T_i}^{(j)}]_2 \quad (11)$$

where $[\hat{\mathbf{y}}_{T_i}^{(j)}]_2$ denotes the second element of a vector $\hat{\mathbf{y}}_{T_i}^{(j)}$. In UniOD, a larger outlier score indicates a higher probability for a data point to be an outlier.

In summary, for each historical dataset (1) we construct multiple graph-structured representations via (2) and (3), and reformulate the outlier-detection problem as a node-classification task. These graphs are then used to train our GNN-based classifier ((6),(7) and (9)) using (10). After training, any new dataset is processed through the same graph-construction pipeline and fed into the pretrained model to assign outlier scores according to (11), thereby identifying outliers in the newly unseen datasets.

3.2.3 Algorithm of UniOD

In this subsection, we provide a detailed algorithm for both the training and testing stages of UniOD in Algorithm 1. Note that to enhance the generalization capability of UniOD, we create 5 synthetic datasets by randomly subsampling 60% samples from each \mathcal{D}_{H_i} , where the outlier (anomaly) ratio remains unchanged from the original dataset. This operation is denoted as *Subsampling*(\mathcal{D}_{H_i}) in Algorithm 1.

3.2.4 Time Complexity Analysis

In this subsection, we compare the time complexity for detecting outliers in \mathcal{D}_{T_i} using the proposed UniOD and other deep learning based methods. For all these deep-learning based methods, assume the maximal hidden dimension of all neural networks is $\tilde{d} > d_{T_i}, d^*$, also we assume the numbers of training epochs and layers of MLP in deep learning based methods except UniOD are Q and L_4 respectively, then the comparison of time complexity on conducting outlier detection experiments in \mathcal{D}_{T_i} between UniOD and two possible upper bounds of these classical deep-learning based methods provided by ICL and DPAD is shown in Table 1, with detailed time complexity for each deep-learning based method provided in *Appendix B*. Also, we compare the number of hyperparameters from

Algorithm 1 Training and Testing Stages of UniOD

Training stage of UniOD:

Input: historical datasets $\mathcal{D}_H = \{\mathcal{D}_{H_1}, \mathcal{D}_{H_2}, \dots, \mathcal{D}_{H_M}\}$, training epoch Q , $\hat{\mathcal{X}}_H = \emptyset$, $\hat{\mathcal{A}}_H = \emptyset$
Output: θ^*

- 1: **for** each historical dataset $\mathcal{D}_{H_i} \in \mathcal{D}_H$ **do**
- 2: $\{\mathcal{D}_{H_i^1}, \mathcal{D}_{H_i^2}, \mathcal{D}_{H_i^3}, \mathcal{D}_{H_i^4}, \mathcal{D}_{H_i^5}\} = \text{Subsampling}(\mathcal{D}_{H_i})$
- 3: Obtain $\hat{\mathcal{A}}_H = \hat{\mathcal{A}}_H \cup \{\mathcal{A}_{H_i^m}\}_{m=1}^5$, $\hat{\mathcal{X}}_H = \hat{\mathcal{X}}_H \cup \{\tilde{X}_{H_i^m}\}_{m=1}^5$ using (2) and (3) respectively.
- 4: **end for**
- 5: Initialize the parameters of UniOD: θ
- 6: **for** $b = 1, \dots, Q$ **do**
- 7: **for** each $\mathbf{X}_{H_i^j} \in \hat{\mathcal{X}}_H$, $\mathcal{A}_{H_i^j} \in \hat{\mathcal{A}}_H$ **do**
- 8: Obtain node classification prediction using (6), (7), (8) and (9)
- 9: Update parameters θ using (10)
- 10: **end for**
- 11: **end for**

Testing stage of UniOD:

Input: newly unseen test dataset \mathcal{D}_{T_i} , trained model parameters θ^*
Output: $\{\text{Outlier Score}(\mathbf{x}_{T_i}^{(j)})\}_{j=1}^{n_{T_i}}$

- 12: Obtain graph structured data $\tilde{X}_{T_i}, \mathcal{A}_{T_i}$ using (2) and (3)
- 13: Obtain outlier score $\{\text{Outlier Score}(\mathbf{x}_{T_i}^{(j)})\}_{j=1}^{n_{T_i}}$ (11) using (6), (7), (8) and (9)

different deep-learning based methods shown in *Appendix C*. In the complexity of the two deep learning based methods, the first and second terms arise from their training process and testing process, respectively. In the complexity of UniOD, the first term arises from calculating output from the GNN-based model, and the second term mainly arises from converting datasets into graphs, including SVD decomposition, the attention part of GT, and the message passing part of GIN. Since the time cost of computing from a neural network can usually be accelerated, the significant time cost may arise from the conversion part. Comparing the complexity of UniOD to all other deep-learning methods, it has several advantages:

- The input dimension of UniOD’s neural network is fixed at d^* , independent of individual dataset dimensions. Consequently, UniOD’s main computational complexity, which is related to GNN, remains constant as dataset dimensionality increases.
- Previously proposed deep-learning based methods require training for each specific dataset, resulting in an increasing number of models and increasing training time as the number of datasets grows.
- In contrast, UniOD uses only one model for all datasets, and its training phase is entirely decoupled from \mathcal{D}_{T_i} , eliminating any need for per-dataset retraining. This decoupling enables UniOD to perform online outlier detection, yielding significantly greater efficiency compared to methods that require both training and testing stages for each dataset.

Table 1: Time complexity comparison in detecting the outliers from a new dataset \mathcal{D}_{T_i} between UniOD and ICL and DPAD, two potential upper bounds of classical deep-learning-based approaches.

	Time Complexity
DPAD	$\mathcal{O}\left(Qn_{T_i}\tilde{d}(L_4\tilde{d} + n_{T_i}) + n_{T_i}\tilde{d}(L_4\tilde{d} + n_{T_i})\right)$
ICL	$\mathcal{O}\left(Qn_{T_i}d_{T_i}L_4\tilde{d}^2 + n_{T_i}d_{T_i}L_4\tilde{d}^2\right)$
UniOD	$\mathcal{O}\left((n_{T_i}(L_1 + L_2 + L_3)\tilde{d}^2 + n_{T_i}^2(\tilde{d} + d_{T_i} + d^*))\right)$

4 Numerical Results

4.1 Experimental Settings

Datasets Our experiments are conducted on ADBench [Han *et al.*, 2022], which is a popular benchmark in outlier (anomaly) detection, containing widely used real-world datasets in multiple domains, including healthcare, audio, language processing, and finance. Detailed descriptions and statistical information about these datasets are provided in the Appendix D.

Baselines UniOD is compared with 15 widely-used baseline methods, including traditional methods: KDE[Parzen, 1962], k NN[Ramaswamy *et al.*, 2000], LOF [Breunig *et al.*, 2000a], OC-SVM[Schölkopf *et al.*, 2001], IF[Liu *et al.*, 2008], ECOD[Li *et al.*, 2022a] and deep-learning based methods: AE [Hinton and Salakhutdinov, 2006], DSVDD[Ruff *et al.*, 2018b], NeutralAD[Qiu *et al.*, 2021], ICL [Shenkar and Wolf, 2022], SLAD[Xu *et al.*, 2023b], DTE[Livernoche *et al.*, 2023b], DPAD[Fu *et al.*, 2024], ODIM[Kim *et al.*, 2024] and KPCA+MLP. For ODIM and DTE, which are proposed for transductive anomaly detection (OD), we report the best-performing results from their original paper. For DPAD, SLAD, ICL, and NeutralAD, we use the code provided by the authors. As for other methods, we use the code from the Python library PyOD [Zhao *et al.*, 2019]. For these methods, we use the best-performing or recommended set of hyperparameters given in their original paper. KPCA+MLP is another baseline method that uses historical labeled datasets for training. It first uses KPCA [Hoffmann, 2007] to obtain uniformly dimensioned data for historical datasets, then uses these historical data to train a MLP as its classifier.

Implementation All of our experiments are implemented using Pytorch [Paszke *et al.*, 2017] on a system equipped with an NVIDIA Tesla A40 GPU and an AMD EPYC 7543 CPU. In UniOD, we set the dimension of unified feature $d^* = 256$, the number of σ is determined as $K = 5$, with $\{\beta_k^2\}_{k=1}^5 = \{0.3, 0.5, 1, 3, 5\}$. Our KGIN $_{\theta_1}$ comprises $L_1 = 4$ layers with successive hidden-dimensionalities [1024, 1024, 1024, 64]. As for KGT $_{\theta_2}$, the dimension of the feedforward network model is set to 1024 and the layer is set to $L_2 = 6$. Classifier MLP $_{\theta_3}$ is a 3-layer MLP with successive hidden-dimensionalities [128, 64, 2]. We use AdamW [Loshchilov and Hutter, 2017] as our optimizer with learning rate being $5 * 10^{-5}$ and weight decay being 10^{-6} to train UniOD for 50 epochs. In our experiments, we use $M = 15$ historical datasets for training, and evaluate the performance of all methods on $B = 15$ different datasets. Each experiment is performed five times to obtain mean value.

Performance Metrics We use two metrics to evaluate the performance of UniOD and other baseline methods: Area Under the Receiver Operating Characteristic Curve (AUROC) and the Area Under the Precision-Recall Curve (AUPRC), following [Xu *et al.*, 2023b; Livernoche *et al.*, 2023b; Kim *et al.*, 2024]. The two metrics are threshold-free and avoid using anomaly ratio of datasets to determine anomaly threshold.

4.2 Results of OD

The average AUROC and AUPRC performance of 16 methods on 15 datasets is shown in Table 2. In AUROC, UniOD achieves the best average performance of 78.9%, which is 2% higher than the second-best method-IF. It is noteworthy that UniOD is the only deep-learning based method that performs better than IF. As for AUPRC, UniOD achieves an average performance of 45.4%, which is only slightly worse than the best method-IF. Compared with KPCA+MLP, which also uses historical datasets, UniOD significantly outperforms KPCA+MLP, illustrating the effectiveness of using graph structure information and graph neural networks (GNNs). Another interesting phenomenon is that simple traditional methods like IF, k NN, and KDE outperform most deep-learning based methods in various datasets, one of the main reasons is that in tabular data with low-dimensional features, even simple Euclidean distance reflects semantic differences between different samples. However, as the number of high-dimensional datasets increases, deep-learning based methods will be more powerful since methods like k NN and KDE provides inexplicit results for high-dimensional datasets as discussed in [Jiang, 2017; Gu *et al.*, 2019].

Also, we compare the time cost of different deep-learning based methods for conducting outlier detection experiments on the 15 datasets, and the results are shown in Table 3. UniOD achieves a lower time cost than several recent proposed deep-learning methods such as SLAD, ICL and NeutralAD. In the analysis of time complexity, we divide the testing complexity of UniOD as two parts, neural-network-computing part and graph-converting part. The first part takes 9 seconds while

Table 2: Average AUROC (%) and AUPRC (%) of each method on 15 tabular datasets of ADBench. The best results are marked in **bold**.

AUROC	KPCA +MLP (2023)	SLAD (2024)	ODIM (2024)	DTE (2024)	DPAD (2024)	ICL (2022)	ECOD (2022)	NeutralAD (2021)	DSVDD (2018)	AE (2006)	OC-SVM (2001)	<i>k</i> NN (2000)	IF (2008)	LOF (2000)	KDE (1962)	UniOD Ours
breastw	28.70	88.60	99.10	97.60	91.30	76.40	99.10	78.10	85.70	96.50	95.10	97.70	98.30	44.90	98.40	99.10
Cardiotocography	42.20	38.70	68.10	49.30	47.00	37.10	78.50	42.30	68.70	54.20	69.60	49.10	68.10	52.40	50.30	51.20
fault	46.50	71.20	56.70	72.60	66.30	67.10	46.90	68.40	51.00	68.60	53.90	72.00	54.40	59.60	73.10	69.60
InternetAds	51.80	61.90	62.50	63.40	56.50	59.20	67.70	65.40	62.40	57.90	61.60	65.20	62.50	60.90	59.50	63.50
landsat	49.50	67.50	46.20	60.20	55.70	64.30	36.80	70.90	39.00	52.60	42.40	57.60	46.20	54.70	62.50	69.10
optdigits	39.80	54.80	58.60	38.60	46.50	53.30	60.50	34.70	33.80	47.20	50.70	37.20	69.60	53.70	32.30	73.80
PageBlocks	66.80	73.50	88.20	90.60	84.60	74.20	91.40	77.70	90.30	88.20	91.50	83.40	88.20	71.60	90.70	88.20
pendigits	62.40	66.60	95.10	78.60	64.90	67.30	92.70	69.20	70.40	77.50	93.10	74.30	94.70	49.90	89.10	77.50
Pima	53.70	51.30	71.90	70.70	65.40	51.50	59.40	57.10	65.30	62.80	62.40	70.90	67.40	60.10	72.30	72.30
satellite	49.90	73.40	69.80	70.20	68.50	60.10	58.30	57.60	62.80	66.70	66.40	66.50	69.50	54.20	76.00	86.90
satimage-2	61.10	94.00	99.80	98.00	77.50	86.50	96.50	70.20	95.60	95.20	99.70	93.20	99.30	53.60	96.40	99.70
SpamBase	9.80	48.20	55.00	54.50	47.40	47.10	65.60	45.30	53.20	54.60	53.40	48.90	63.70	45.70	49.50	56.30
thyroid	73.00	80.90	91.60	96.40	84.50	73.20	97.70	64.50	91.40	94.10	95.90	95.90	97.90	66.50	95.80	94.10
Waveform	51.30	44.80	72.20	72.90	64.80	63.20	60.30	72.10	63.60	62.40	67.20	72.30	70.70	70.60	75.10	84.30
WDBC	58.50	87.60	97.70	97.50	83.70	75.10	97.10	26.90	97.70	94.40	98.30	97.40	98.80	98.20	95.00	98.40
Average Value	53.80	66.87	75.50	74.07	66.97	63.70	73.90	60.03	68.73	71.53	73.41	72.11	76.62	59.77	74.40	78.93
AUPRC																
breastw	26.90	78.40	98.80	92.10	77.70	75.70	98.30	53.50	84.60	90.50	91.70	92.30	96.20	29.70	95.50	96.90
Cardiotocography	22.60	23.60	38.90	31.20	25.00	16.60	50.50	21.20	42.70	30.00	41.30	28.60	43.50	27.50	27.50	35.30
fault	31.40	51.90	44.40	53.20	48.40	45.30	32.50	49.20	36.90	51.50	40.10	52.90	39.70	39.60	54.50	49.10
InternetAds	20.00	26.90	23.40	29.00	24.20	25.10	50.80	27.80	30.20	22.00	29.20	27.90	47.00	24.20	22.60	32.80
landsat	18.80	30.30	17.90	25.50	23.10	46.30	16.30	34.60	18.70	22.20	17.50	24.70	19.20	25.10	26.00	28.10
optdigits	2.20	2.90	3.00	2.10	2.60	3.02	3.30	2.00	2.00	2.50	2.60	2.20	4.70	3.50	1.90	5.00
PageBlocks	20.10	39.00	50.90	53.00	47.10	29.10	51.90	26.50	54.40	38.80	53.30	46.90	47.00	29.40	53.90	46.20
pendigits	2.70	4.90	30.20	8.90	5.00	2.80	26.50	4.30	9.20	5.50	22.70	7.50	26.00	4.30	12.10	6.00
Pima	37.40	36.50	49.10	52.80	48.10	36.40	46.40	38.60	49.50	44.60	46.30	52.90	50.20	41.80	53.40	52.90
satellite	29.30	51.00	65.20	56.30	50.40	46.80	52.60	40.30	58.10	53.60	65.50	51.80	64.90	37.20	60.30	79.20
satimage-2	1.40	27.80	94.90	50.70	4.50	10.30	65.90	2.19	56.30	32.20	96.50	34.70	91.60	3.10	31.80	95.70
SpamBase	49.80	37.60	41.00	40.70	38.20	31.30	51.80	37.40	39.70	40.90	40.20	39.40	48.70	35.90	38.20	42.50
thyroid	13.10	17.70	32.70	36.00	14.90	5.70	46.70	3.40	20.90	41.10	31.80	27.30	49.30	7.30	28.60	44.30
Waveform	2.70	2.40	5.30	10.90	6.00	7.60	4.00	27.20	5.00	5.30	5.20	10.50	4.70	7.50	11.40	9.60
WDBC	3.40	23.50	61.20	46.50	18.10	5.70	50.50	1.90	53.40	30.70	49.30	41.60	55.30	47.80	25.40	57.80
Average Value	18.79	30.33	43.79	39.26	28.93	25.88	43.26	24.71	37.50	34.15	42.25	36.12	45.89	24.30	36.26	45.43

the second part takes 231 seconds, which aligns with our conclusion that a significant time cost may arise from the conversion part.

Table 3: OD Time cost (s) of different deep-learning based methods for 15 datasets, with batch size and training epochs kept constant.

Time Cost	SLAD (2023)	DPAD (2024)	ICL (2022)	NeutralAD (2021)	DSVDD (2018)	AE (2006)	UniOD Ours
	485	788	1391	664	511	384	240

4.3 Ablation Studies

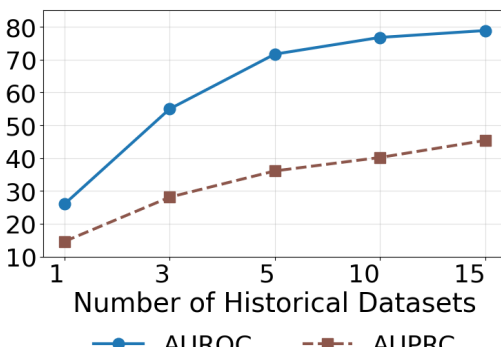


Figure 3: Average AUROC (%) and AUPRC (%) values of UniOD across 15 datasets using different numbers of historical datasets for training.

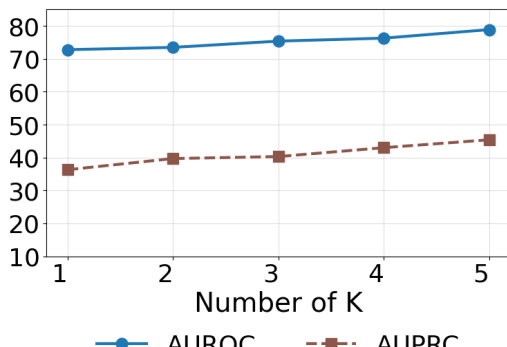


Figure 4: Average AUROC (%) and AUPRC (%) values of UniOD across 15 datasets using different numbers of bandwidth for graph converting.

In this subsection, we conduct external experiments to investigate how each component of our proposed UniOD affects its outlier detection performance. We first evaluate the performance of UniOD with 1, 3, 5, 10, 15 training historical datasets shown in Figure 3. It is obvious that when the number of historical datasets is limited to 5, UniOD's generalization capability is constrained; however, as the number of historical datasets expands, its generalization performance correspondingly

improves. In Figure 4, we analysis how the number of bandwidths for graph converting K impacts the performance of UniOD. Although the impact of K is not as significant as the number of historical datasets, using more bandwidths results in less information loss in the graph conversion process, which improves the generalization ability and performance of UniOD. For more detailed results of ablation studies, please refer to *Appendix E*.

5 Conclusion

We propose a novel yet efficient method for outlier detection called UniOD. The main purpose of UniOD is to leverage information from historical datasets to train a deep learning-based universal model capable of detecting outliers for any newly unseen datasets from different domains without training. Converting each dataset into graph-structured data and generating uniformly dimensioned node features allows UniOD to handle different datasets with one universal model. We provide time complexity analysis for different deep-learning methods and numerical results illustrated the effectiveness and efficiency of UniOD. Although UniOD is primarily proposed for outlier detection (transductive anomaly detection), it can also be used for inductive anomaly detection. In this case, we convert the whole training set and each testing point into graph-structured data and obtain their outlier score. Also, UniOD be applied to other non-tabular type data, such as images, text, and graphs, by simply using existing pre-trained feature extractors to convert the data into vectors.

References

Mohiuddin Ahmed, Abdun Naser Mahmood, and Md Rafiqul Islam. A survey of anomaly detection techniques in financial domain. *Future Generation Computer Systems*, 55:278–288, 2016.

Jerome Andrews, Thomas Tanay, Edward J Morton, and Lewis D Griffin. Transfer representation-learning for anomaly detection. *JMLR*, 2016.

Jens Behrmann, Paul Vicol, Kuan-Chieh Wang, Roger Grosse, and Jörn-Henrik Jacobsen. Understanding and mitigating exploding inverses in invertible neural networks. In *International Conference on Artificial Intelligence and Statistics*, pages 1792–1800. PMLR, 2021.

Liron Bergman and Yedid Hoshen. Classification-based anomaly detection for general data. *arXiv preprint arXiv:2005.02359*, 2020.

Jakub Breier and Jana Branišová. A dynamic rule creation based anomaly detection method for identifying security breaches in log records. *Wireless Personal Communications*, 94:497–511, 2017.

Markus M Breunig, Hans-Peter Kriegel, Raymond T Ng, and Jörg Sander. Lof: identifying density-based local outliers. In *Proceedings of the 2000 ACM SIGMOD international conference on Management of data*, pages 93–104, 2000.

Markus M Breunig, Hans-Peter Kriegel, Raymond T Ng, and Jörg Sander. Lof: identifying density-based local outliers. In *Proceedings of the 2000 ACM SIGMOD international conference on Management of data*, pages 93–104, 2000.

Jinyu Cai and Jicong Fan. Perturbation learning based anomaly detection. In S. Koyejo, S. Mohamed, A. Agarwal, D. Belgrave, K. Cho, and A. Oh, editors, *Advances in Neural Information Processing Systems*, volume 35, pages 14317–14330. Curran Associates, Inc., 2022.

Varun Chandola, Arindam Banerjee, and Vipin Kumar. Anomaly detection: A survey. *ACM computing surveys (CSUR)*, 41(3):1–58, 2009.

Yuanhong Chen, Yu Tian, Guansong Pang, and Gustavo Carneiro. Deep one-class classification via interpolated gaussian descriptor. In *Proceedings of the AAAI Conference on Artificial Intelligence*, volume 36, pages 383–392, 2022.

Sihan Chen, Zhuangzhuang Qian, Wingchun Siu, Xingcan Hu, Jiaqi Li, Shawn Li, Yuehan Qin, Tiankai Yang, Zhuo Xiao, Wanghao Ye, et al. Pyod 2: A python library for outlier detection with l1m-powered model selection. *arXiv preprint arXiv:2412.12154*, 2024.

Sihan Chen, Zhuangzhuang Qian, Wingchun Siu, Xingcan Hu, Jiaqi Li, Shawn Li, Yuehan Qin, Tiankai Yang, Zhuo Xiao, Wanghao Ye, Yichi Zhang, Yushun Dong, and Yue Zhao. Pyod 2: A python library for outlier detection with llm-powered model selection. *arXiv preprint arXiv:2412.12154*, 2024.

Wei Dai and Jicong Fan. AutoUAD: Hyper-parameter optimization for unsupervised anomaly detection. In *The Thirteenth International Conference on Learning Representations*, 2025.

Lucas Deecke, Robert Vandermeulen, Lukas Ruff, Stephan Mandt, and Marius Kloft. Image anomaly detection with generative adversarial networks. In *Machine Learning and Knowledge Discovery in Databases: European Conference, ECML PKDD 2018, Dublin, Ireland, September 10–14, 2018, Proceedings, Part I 18*, pages 3–17. Springer, 2019.

Xueying Ding, Lingxiao Zhao, and Leman Akoglu. Hyperparameter sensitivity in deep outlier detection: Analysis and a scalable hyper-ensemble solution. *Advances in Neural Information Processing Systems*, 35:9603–9616, 2022.

Laurent Dinh, Jascha Sohl-Dickstein, and Samy Bengio. Density estimation using real nvp. *arXiv preprint arXiv:1605.08803*, 2016.

Min Du, Feifei Li, Guineng Zheng, and Vivek Srikumar. Deeplog: Anomaly detection and diagnosis from system logs through deep learning. In *Proceedings of the 2017 ACM SIGSAC conference on computer and communications security*, pages 1285–1298, 2017.

Dazhi Fu, Zhao Zhang, and Jicong Fan. Dense projection for anomaly detection. In *Proceedings of the AAAI Conference on Artificial Intelligence*, volume 38, pages 8398–8408, 2024.

Markus Goldstein and Seiichi Uchida. A comparative evaluation of unsupervised anomaly detection algorithms for multivariate data. *PloS one*, 11(4):e0152173, 2016.

Ian J Goodfellow, Jean Pouget-Abadie, Mehdi Mirza, Bing Xu, David Warde-Farley, Sherjil Ozair, Aaron Courville, and Yoshua Bengio. Generative adversarial nets. *Advances in neural information processing systems*, 27, 2014.

Sachin Goyal, Aditi Raghunathan, Moksh Jain, Harsha Vardhan Simhadri, and Prateek Jain. Droc: Deep robust one-class classification. In *International conference on machine learning*, pages 3711–3721. PMLR, 2020.

Xiaoyi Gu, Leman Akoglu, and Alessandro Rinaldo. Statistical analysis of nearest neighbor methods for anomaly detection. *Advances in Neural Information Processing Systems*, 32, 2019.

Denis Gudovskiy, Shun Ishizaka, and Kazuki Kozuka. Cflow-ad: Real-time unsupervised anomaly detection with localization via conditional normalizing flows. In *Proceedings of the IEEE/CVF winter conference on applications of computer vision*, pages 98–107, 2022.

Songqiao Han, Xiyang Hu, Hailiang Huang, Minqi Jiang, and Yue Zhao. Adbench: Anomaly detection benchmark. *Advances in Neural Information Processing Systems*, 35:32142–32159, 2022.

Geoffrey E Hinton and Ruslan R Salakhutdinov. Reducing the dimensionality of data with neural networks. *science*, 313(5786):504–507, 2006.

Victoria Hodge and Jim Austin. A survey of outlier detection methodologies. *Artificial intelligence review*, 22:85–126, 2004.

Heiko Hoffmann. Kernel pca for novelty detection. *Pattern recognition*, 40(3):863–874, 2007.

Aapo Hyvärinen and Hiroshi Morioka. Unsupervised feature extraction by time-contrastive learning and nonlinear ica. *Advances in neural information processing systems*, 29, 2016.

Aapo Hyvärinen and Erkki Oja. Independent component analysis: algorithms and applications. *Neural networks*, 13(4-5):411–430, 2000.

Aapo Hyvärinen and Petteri Pajunen. Nonlinear independent component analysis: Existence and uniqueness results. *Neural networks*, 12(3):429–439, 1999.

Aapo Hyvärinen, Jarmo Hurri, Patrik O Hoyer, Aapo Hyvärinen, Jarmo Hurri, and Patrik O Hoyer. *Independent component analysis*. Springer, 2009.

Aapo Hyvärinen, Hiroaki Sasaki, and Richard Turner. Nonlinear ica using auxiliary variables and generalized contrastive learning. In *The 22nd International Conference on Artificial Intelligence and Statistics*, pages 859–868. PMLR, 2019.

Heinrich Jiang. Uniform convergence rates for kernel density estimation. In *International Conference on Machine Learning*, pages 1694–1703. PMLR, 2017.

Mahyar Khayatkhoei, Maneesh K Singh, and Ahmed Elgammal. Disconnected manifold learning for generative adversarial networks. *Advances in Neural Information Processing Systems*, 31, 2018.

Daehyun Kim, Sungyong Baik, and Tae Hyun Kim. Sanflow: Semantic-aware normalizing flow for anomaly detection. *Advances in Neural Information Processing Systems*, 36:75434–75454, 2023.

Dongha Kim, Jaesung Hwang, Jongjin Lee, Kunwoong Kim, and Yongdai Kim. Odim: Outlier detection via likelihood of under-fitted generative models. In *International Conference on Machine Learning*, pages 23941–23971. PMLR, 2024.

Polina Kirichenko, Pavel Izmailov, and Andrew G Wilson. Why normalizing flows fail to detect out-of-distribution data. *Advances in neural information processing systems*, 33:20578–20589, 2020.

Ivan Kobyzev, Simon JD Prince, and Marcus A Brubaker. Normalizing flows: An introduction and review of current methods. *IEEE transactions on pattern analysis and machine intelligence*, 43(11):3964–3979, 2020.

Zheng Li, Yue Zhao, Xiyang Hu, Nicola Botta, Cezar Ionescu, and George H Chen. Ecod: Unsupervised outlier detection using empirical cumulative distribution functions. *IEEE Transactions on Knowledge and Data Engineering*, 35(12):12181–12193, 2022.

Zheng Li, Yue Zhao, Xiyang Hu, Nicola Botta, Cezar Ionescu, and George H Chen. Ecod: Unsupervised outlier detection using empirical cumulative distribution functions. *IEEE Transactions on Knowledge and Data Engineering*, 35(12):12181–12193, 2022.

Fei Tony Liu, Kai Ming Ting, and Zhi-Hua Zhou. Isolation forest. In *2008 eighth ieee international conference on data mining*, pages 413–422. IEEE, 2008.

Boyang Liu, Pang-Ning Tan, and Jiayu Zhou. Unsupervised anomaly detection by robust density estimation. In *Proceedings of the AAAI Conference on Artificial Intelligence*, volume 36, pages 4101–4108, 2022.

Jing Liu, Zhenchao Ma, Zepu Wang, Chenxuanyin Zou, Jiayang Ren, Zehua Wang, Liang Song, Bo Hu, Yang Liu, and Victor Leung. A survey on diffusion models for anomaly detection. *arXiv preprint arXiv:2501.11430*, 2025.

Victor Livernoche, Vineet Jain, Yashar Hezaveh, and Siamak Ravanbakhsh. On diffusion modeling for anomaly detection. *arXiv preprint arXiv:2305.18593*, 2023.

Victor Livernoche, Vineet Jain, Yashar Hezaveh, and Siamak Ravanbakhsh. On diffusion modeling for anomaly detection. *arXiv preprint arXiv:2305.18593*, 2023.

Ilya Loshchilov and Frank Hutter. Decoupled weight decay regularization. *arXiv preprint arXiv:1711.05101*, 2017.

David F Nettleton, Albert Orriols-Puig, and Albert Fornells. A study of the effect of different types of noise on the precision of supervised learning techniques. *Artificial intelligence review*, 33:275–306, 2010.

Guansong Pang, Chunhua Shen, and Anton Van Den Hengel. Deep anomaly detection with deviation networks. In *Proceedings of the 25th ACM SIGKDD international conference on knowledge discovery & data mining*, pages 353–362, 2019.

Guansong Pang, Chunhua Shen, Longbing Cao, and Anton Van Den Hengel. Deep learning for anomaly detection: A review. *ACM computing surveys (CSUR)*, 54(2):1–38, 2021.

Emanuel Parzen. On estimation of a probability density function and mode. *The annals of mathematical statistics*, 33(3):1065–1076, 1962.

Adam Paszke, Sam Gross, Soumith Chintala, Gregory Chanan, Edward Yang, Zachary DeVito, Zeming Lin, Alban Desmaison, Luca Antiga, and Adam Lerer. Automatic differentiation in pytorch. 2017.

Pramuditha Perera, Ramesh Nallapati, and Bing Xiang. Ocgan: One-class novelty detection using gans with constrained latent representations. In *Proceedings of the IEEE/CVF conference on computer vision and pattern recognition*, pages 2898–2906, 2019.

Marco AF Pimentel, David A Clifton, Lei Clifton, and Lionel Tarassenko. A review of novelty detection. *Signal processing*, 99:215–249, 2014.

Yuehan Qin, Yichi Zhang, Yi Nian, Xueying Ding, and Yue Zhao. Metaood: Automatic selection of ood detection models. *arXiv preprint arXiv:2410.03074*, 2024.

Chen Qiu, Timo Pfommer, Marius Kloft, Stephan Mandt, and Maja Rudolph. Neural transformation learning for deep anomaly detection beyond images. In *International conference on machine learning*, pages 8703–8714. PMLR, 2021.

Sridhar Ramaswamy, Rajeev Rastogi, and Kyuseok Shim. Efficient algorithms for mining outliers from large data sets. In *Proceedings of the 2000 ACM SIGMOD international conference on Management of data*, pages 427–438, 2000.

Amit Rozner, Barak Battash, Henry Li, Lior Wolf, and Ofir Lindenbaum. Anomaly detection with variance stabilized density estimation. *arXiv preprint arXiv:2306.00582*, 2023.

Lukas Ruff, Robert Vandermeulen, Nico Goernitz, Lucas Deecke, Shoaib Ahmed Siddiqui, Alexander Binder, Emmanuel Müller, and Marius Kloft. Deep one-class classification. In *International conference on machine learning*, pages 4393–4402. PMLR, 2018.

Lukas Ruff, Robert Vandermeulen, Nico Goernitz, Lucas Deecke, Shoaib Ahmed Siddiqui, Alexander Binder, Emmanuel Müller, and Marius Kloft. Deep one-class classification. In *International conference on machine learning*, pages 4393–4402. PMLR, 2018.

Lukas Ruff, Robert A Vandermeulen, Nico Görnitz, Alexander Binder, Emmanuel Müller, Klaus-Robert Müller, and Marius Kloft. Deep semi-supervised anomaly detection. *arXiv preprint arXiv:1906.02694*, 2019.

Lukas Ruff, Jacob R Kauffmann, Robert A Vandermeulen, Grégoire Montavon, Wojciech Samek, Marius Kloft, Thomas G Dietterich, and Klaus-Robert Müller. A unifying review of deep and shallow anomaly detection. *Proceedings of the IEEE*, 109(5):756–795, 2021.

Thomas Schlegl, Philipp Seeböck, Sebastian M Waldstein, Georg Langs, and Ursula Schmidt-Erfurth. f-anogan: Fast unsupervised anomaly detection with generative adversarial networks. *Medical image analysis*, 54:30–44, 2019.

Bernhard Schölkopf, John C Platt, John Shawe-Taylor, Alex J Smola, and Robert C Williamson. Estimating the support of a high-dimensional distribution. *Neural computation*, 13(7):1443–1471, 2001.

Tom Shenkar and Lior Wolf. Anomaly detection for tabular data with internal contrastive learning. In *International conference on learning representations*, 2022.

Karanjit Singh and Shuchita Upadhyaya. Outlier detection: applications and techniques. *International Journal of Computer Science Issues (IJCSI)*, 9(1):307, 2012.

Yiyou Sun, Yifei Ming, Xiaojin Zhu, and Yixuan Li. Out-of-distribution detection with deep nearest neighbors. In *International Conference on Machine Learning*, pages 20827–20840. PMLR, 2022.

Jan Van Haaren, Andrey Kolobov, and Jesse Davis. Todtler: Two-order-deep transfer learning. In *Proceedings of the AAAI Conference on Artificial Intelligence*, volume 29, 2015.

Vincent Vercruyssen, Wannes Meert, and Jesse Davis. Transfer learning for time series anomaly detection. In *Proceedings of the Workshop and Tutorial on Interactive Adaptive Learning@ ECMLPKDD 2017*, volume 1924, pages 27–37. CEUR Workshop Proceedings, 2017.

Vercruyssen Vincent, Meert Wannes, and Davis Jesse. Transfer learning for anomaly detection through localized and unsupervised instance selection. In *Proceedings of the AAAI Conference on Artificial Intelligence*, volume 34, pages 6054–6061, 2020.

Shaoyu Wang, Xinyu Wang, Liangpei Zhang, and Yanfei Zhong. Auto-ad: Autonomous hyperspectral anomaly detection network based on fully convolutional autoencoder. *IEEE Transactions on Geoscience and Remote Sensing*, 60:1–14, 2021.

Karl Weiss, Taghi M Khoshgoftaar, and DingDing Wang. A survey of transfer learning. *Journal of Big data*, 3:1–40, 2016.

David H Wolpert and William G Macready. No free lunch theorems for optimization. *IEEE transactions on evolutionary computation*, 1(1):67–82, 1997.

Xuan Xia, Xizhou Pan, Nan Li, Xing He, Lin Ma, Xiaoguang Zhang, and Ning Ding. Gan-based anomaly detection: A review. *Neurocomputing*, 493:497–535, 2022.

Yanshan Xiao, Bo Liu, Philip S Yu, and Zhifeng Hao. A robust one-class transfer learning method with uncertain data. *Knowledge and Information Systems*, 44:407–438, 2015.

Keyulu Xu, Weihua Hu, Jure Leskovec, and Stefanie Jegelka. How powerful are graph neural networks? *arXiv preprint arXiv:1810.00826*, 2018.

Hongzuo Xu, Guansong Pang, Yijie Wang, and Yongjun Wang. Deep isolation forest for anomaly detection. *IEEE Transactions on Knowledge and Data Engineering*, 35(12):12591–12604, 2023.

Hongzuo Xu, Yijie Wang, Juhui Wei, Songlei Jian, Yizhou Li, and Ning Liu. Fascinating supervisory signals and where to find them: Deep anomaly detection with scale learning. In *International Conference on Machine Learning*, pages 38655–38673. PMLR, 2023.

Jiawei Yu, Ye Zheng, Xiang Wang, Wei Li, Yushuang Wu, Rui Zhao, and Liwei Wu. Fastflow: Unsupervised anomaly detection and localization via 2d normalizing flows. *arXiv preprint arXiv:2111.07677*, 2021.

Yunhe Zhang, Yan Sun, Jinyu Cai, and Jicong Fan. Deep orthogonal hypersphere compression for anomaly detection. In *The Twelfth International Conference on Learning Representations*, 2024.

Yue Zhao and Leman Akoglu. Hyperparameter optimization for unsupervised outlier detection. *arXiv preprint arXiv:2208.11727*, 2022.

Yue Zhao, Zain Nasrullah, and Zheng Li. Pyod: A python toolbox for scalable outlier detection. *Journal of machine learning research*, 20(96):1–7, 2019.

Yue Zhao, Ryan A Rossi, and Leman Akoglu. Automating outlier detection via meta-learning. *arXiv preprint arXiv:2009.10606*, 2020.

Yue Zhao, Sean Zhang, and Leman Akoglu. Toward unsupervised outlier model selection. In *2022 IEEE International Conference on Data Mining (ICDM)*, pages 773–782. IEEE, 2022.

Yujia Zheng, Ignavier Ng, and Kun Zhang. On the identifiability of nonlinear ica: Sparsity and beyond. *Advances in neural information processing systems*, 35:16411–16422, 2022.

Bo Zong, Qi Song, Martin Renqiang Min, Wei Cheng, Cristian Lumezanu, Daeki Cho, and Haifeng Chen. Deep autoencoding gaussian mixture model for unsupervised anomaly detection. In *International conference on learning representations*, 2018.

Table 4: Time complexity comparison of UniOD and classical deep learning based methods in detecting the outliers of a new dataset \mathcal{D}_{T_i} .

	Time Complexity
SLAD	$\mathcal{O}(Qn_{T_i}r(c+1)L_4\tilde{d}^2 + n_{T_i}r(c+1)L_4\tilde{d}^2)$
DPAD	$\mathcal{O}(Q(n_{T_i}L_4\tilde{d}^2 + n_{T_i}^2\tilde{d}) + (n_{T_i}L_4\tilde{d}^2 + n_{T_i}^2\tilde{d}))$
ICL	$\mathcal{O}(Qn_{T_i}(d_{T_i}-k+1)L_4\tilde{d}^2 + (n_{T_i}(d_{T_i}-k+1)L_4\tilde{d}^2))$
NeutralAD	$\mathcal{O}(2Qn_{T_i}eL_4\tilde{d}^2 + 2n_{T_i}eL_4\tilde{d}^2)$
DSVDD	$\mathcal{O}(3Qn_{T_i}L_4\tilde{d}^2 + n_{T_i}L_4\tilde{d}^2)$
AE	$\mathcal{O}(2Qn_{T_i}L_4\tilde{d}^2 + 2n_{T_i}L_4\tilde{d}^2)$
UniOD	$\mathcal{O}((n_{T_i}(L_1+L_2+L_3)\tilde{d}^2 + n_{T_i}^2(\tilde{d}+d_{T_i}+d^*)))$

Table 5: The number of hyperparameters in recent deep-learning based methods.

Methods	Hyperparameters	Number
ODIM	K, N_u, N_{pat}	3
SLAD	$h, c, r, \delta, \gamma,$	5
DPAD	γ, λ, k	3
ICL	k, u, τ, r	4
NeutralAD	τ, K, m	3
UniOD	-	0

A Algorithm Details

A.1 KGIN $_{\theta_1}$ and KGT $_{\theta_2}$

KGIN $_{\theta_1}$ and KGT $_{\theta_2}$ are combinations of K GINs and GTs respectively. For the k -th GIN GIN $_{\theta_1}^k$ and GT $_{\theta_2}^k$ parameterized by θ_1^k, θ_2^k , their outputs follows:

$$\begin{aligned} \mathbf{Z}_{H_i}^{\text{GIN}_k} &= \text{GIN}_{\theta_1^k} \left(\tilde{\mathbf{X}}_{H_i}, \mathcal{A}_{H_i} \right), \quad i = 1, \dots, M \\ \mathbf{Z}_{H_i}^{\text{GT}_k} &= \text{GT}_{\theta_2^k} \left(\tilde{\mathbf{X}}_{H_i} \right), \quad i = 1, \dots, M \end{aligned} \quad (12)$$

Then, we have $\mathbf{Z}_{H_i}^{\text{GIN}}$ and $\mathbf{Z}_{H_i}^{\text{GT}}$ follows:

$$\begin{aligned} \mathbf{Z}_{H_i}^{\text{GIN}} &= [\mathbf{Z}_{H_i}^{\text{GIN}_1}, \mathbf{Z}_{H_i}^{\text{GIN}_2}, \dots, \mathbf{Z}_{H_i}^{\text{GIN}_K}], \theta_1 = \{\theta_1^k\}_{k=1}^K \\ \mathbf{Z}_{H_i}^{\text{GT}} &= [\mathbf{Z}_{H_i}^{\text{GT}_1}, \mathbf{Z}_{H_i}^{\text{GT}_2}, \dots, \mathbf{Z}_{H_i}^{\text{GT}_K}], \theta_2 = \{\theta_2^k\}_{k=1}^K \end{aligned} \quad (13)$$

A.2 GIN

The details about GIN are as follows:

$$\forall l \in [1, 2, \dots, L-1], h^{(j),l+1} = f_{\Theta^{(l+1)}} \left((1 + \epsilon)h^{(j),l} + \sum_{u \in \mathcal{N}(j)} A h^{(u),l} \right) \quad (14)$$

where $h^{(j),l+1}$ is the output from $l+1$ GIN layer, $h^{(j),0} = \tilde{\mathbf{x}}_{H_i, \sigma_k}^{(j)}$ is the input node feature, $\mathcal{N}(j)$ denotes the neighbor set of node j , $f_{\Theta^{(l+1)}}$ is a multi layer perceptrons (MLP) parameterized by $\Theta^{(l+1)}$, ϵ_k is a learnable parameter.

Table 6: Statistics of 30 real-world datasets in ADBench.

Data	# Samples	# Features	# Outlier	% Outlier Ratio	Category	Historical
ALOI	49534	27	1508	3.04	Image	✓
campaign	41188	62	4640	11.27	Finance	✓
cardio	1831	21	176	9.61	Healthcare	✓
celeba	202599	39	4547	2.24	Image	✓
cover	286048	10	2747	0.96	Botany	✓
Wilt	4819	5	257	5.33	Botany	✓
http	567498	3	2211	0.39	Web	✓
letter	1600	32	100	6.25	Image	✓
magic.gamma	19020	10	6688	35.16	Physical	✓
mammography	11183	6	260	2.32	Healthcare	✓
shuttle	49097	9	3511	7.15	Astronautics	✓
skin	245057	3	50859	20.75	Image	✓
smtp	95156	3	30	0.03	Web	✓
speech	3686	400	61	1.65	Linguistics	✓
vowels	1456	12	50	3.43	Linguistics	✓
breastw	683	9	239	34.99	Healthcare	✗
Cardiotocography	2114	21	466	22.04	Healthcare	✗
fault	1941	27	673	34.67	Physical	✗
InternetAds	1966	1555	368	18.72	Image	✗
landsat	6435	36	1333	20.71	Astronautics	✗
optdigits	5216	64	150	2.88	Image	✗
PageBlocks	5393	10	510	9.46	Document	✗
pendigits	6870	16	156	2.27	Image	✗
Pima	768	8	268	34.90	Healthcare	✗
satellite	6435	36	2036	31.64	Astronautics	✗
SpamBase	4207	57	1679	39.91	Document	✗
satimage-2	5803	36	71	1.22	Astronautics	✗
thyroid	3772	6	93	2.47	Healthcare	✗
Waveform	3443	21	100	2.90	Physics	✗
WDBC	367	30	10	2.72	Healthcare	✗

B Detailed Complexity Comparison for Deep-Learning based OD methods

In this section, we analysis the time complexity on conducting outlier detection for each deep-learning based methods. For all these methods which primarily uses MLP in the form of encoder, we assume that the largest hidden dimension is \tilde{d} , the training epoch is Q and the layer of this encoder is L_4 , for those methods using decoder as well, we assume the layer of encoder is equal to L_4 . The time complexity comparison of conducting outlier detection on a new dataset \mathcal{D}_{T_i} between several deep-learning based methods is shown in Table 4. Note that here we assume Several specific parameters for these models are:

- SLAD: SLAD includes two hyperparamters r, c which defines the repeat time for data trnasformation and the number of sub-vectors.
- ICL: ICL includes a hyperparamter $0 < q \leq d_{T_i}$ which splits each data into $d_{T_i} - k + 1$ pairs.
- NeutralAD: NeutralAD includes a hyperparamter e which determines the number of learnable transformations.
- DSVDD: DSVDD requires using AE to pretrain its encoder.

C Hyperparameter Comparison of OD Methods

Most deep-learning based OD methods have several hyperparameters which can significantly affect their performance. In Table 5, we compare the number of hyperparameters of different deep-learning based methods. Notably, classical deep-learning methods require careful tuning of at least 3 hyperparameters. In contrast, UniOD involves no hyperparameters in its objective learning except the network architecture design, which is also involved in all other deep-learning based methods.

Table 7: Average AUROC (%) and AUPRC (%) of UniOD on 15 tabular datasets of ADBench using different numbers K of bandwidth for graph converting.

AUROC	$K = 1$	$K = 2$	$K = 3$	$K = 4$	$K = 5$
breastw	96.73	96.83	77.35	98.36	99.10
Cardiotocography	44.49	41.76	49.69	47.21	51.20
fault	55.73	71.06	66.86	66.15	69.60
InternetAds	60.50	60.56	62.84	62.19	63.50
landsat	66.20	61.47	63.53	63.93	69.10
optdigits	81.61	71.68	60.58	58.88	73.80
PageBlocks	93.46	94.55	85.88	87.48	88.20
pendigits	53.94	78.17	88.41	85.06	77.50
Pima	70.72	74.34	73.66	72.80	72.30
satellite	84.59	81.13	82.48	82.62	86.90
satimage-2	64.63	78.97	99.81	99.76	99.70
SpamBase	56.51	57.05	55.29	56.01	56.30
thyroid	97.69	96.23	90.70	96.94	94.10
Waveform	79.30	81.85	79.57	80.32	84.30
WDBC	87.20	74.90	95.29	97.17	98.40
AVG	72.89	74.70	75.46	76.99	78.93
AUPRC					
breastw	92.75	90.20	93.02	97.69	96.90
Cardiotocography	26.90	26.84	28.54	36.30	35.30
fault	42.14	53.49	52.78	45.45	49.10
InternetAds	29.07	30.52	30.36	29.94	32.80
landsat	26.90	24.84	29.80	20.84	28.10
optdigits	6.81	4.57	4.04	3.10	5.00
PageBlocks	57.53	73.25	45.73	43.95	46.20
pendigits	3.34	4.54	4.89	7.85	6.00
Pima	51.02	54.62	54.75	52.42	52.90
satellite	78.03	76.59	81.47	70.82	79.20
satimage-2	7.97	19.50	49.60	96.24	95.70
SpamBase	42.92	44.22	42.26	41.07	42.50
thyroid	55.81	49.82	42.19	37.69	44.30
Waveform	8.40	16.87	14.94	6.96	9.60
WDBC	15.52	39.68	41.25	55.11	57.80
AVG	36.34	40.64	41.04	43.03	45.43

D Statistics of Datasets

In our experiments, we train our model using 15 historical datasets and evaluate the performance of 16 methods on 15 widely used real-world datasets spanning multiple domains, including healthcare, audio, language processing, and finance, in a popular benchmark for anomaly detection Han *et al.* [2022]. The statistics of these datasets are shown in Table 6. These datasets encompass a range of samples and features, from small to large, providing comprehensive metrics and evaluations for the methods.

E Detailed Results for Ablation Studies

In this section, we provide more detailed experimental results for ablation studies.

E.1 Results of Using Multiply Band Width for Graph Converting

Table 7 provide the OD performance results of UniOD on 15 tabular datasets of ADBench using different numbers K of bandwidth for graph converting. As shown in the table, when we use multiple

band width for graph converting, the detection performance and generalization ability increases significantly which mainly stems from less information loss of these datasets.

E.2 Results of Using Different Numbers of Historical Datasets

Table 8: Average AUROC (%) and AUPRC (%) of UniOD on 15 tabular datasets of ADBench using different numbers M of historical datasets for training.

AUROC	$M = 1$	$M = 3$	$M = 5$	$M = 10$	$M = 15$
breastw	84.59	15.39	70.53	98.39	99.10
Cardiotocography	28.37	64.32	57.71	61.71	51.20
fault	51.99	48.67	67.90	56.17	69.60
InternetAds	39.74	61.57	62.53	61.83	63.50
landsat	43.63	55.51	66.89	60.28	69.10
optdigits	43.15	70.63	66.30	62.65	73.80
PageBlocks	20.66	88.03	76.74	89.66	88.20
pendigits	7.19	56.70	79.32	87.98	77.50
Pima	37.73	67.64	72.58	71.18	72.30
satellite	28.42	76.14	84.95	80.18	86.90
satimage-2	7.10	98.12	99.65	99.84	99.70
SpamBase	53.85	56.11	55.42	55.60	56.30
thyroid	14.78	85.55	95.82	96.66	94.10
Waveform	31.75	61.11	77.37	81.22	84.30
WDBC	14.79	95.10	98.60	96.67	98.40
AVG	33.85	66.71	75.49	77.33	78.93
AUPRC					
breastw	60.13	33.80	75.76	95.80	96.90
Cardiotocography	14.70	39.23	37.57	38.11	35.30
fault	34.20	31.96	48.42	42.63	49.10
InternetAds	16.35	33.11	30.88	29.74	32.80
landsat	17.39	23.01	27.22	24.05	28.10
optdigits	2.31	5.07	3.82	3.46	5.00
PageBlocks	5.57	45.37	24.62	45.44	46.20
pendigits	1.21	4.25	5.05	8.45	6.00
Pima	30.47	49.20	53.20	53.63	52.90
satellite	22.04	74.01	79.25	75.38	79.20
satimage-2	0.65	58.84	92.87	96.69	95.70
SpamBase	48.92	42.50	41.31	41.05	42.50
thyroid	1.37	34.75	35.75	35.44	44.30
Waveform	1.94	3.55	6.22	9.00	9.60
WDBC	1.72	25.55	59.87	33.19	57.80
AVG	17.26	33.61	41.45	42.14	45.43

Table 8 presents the outlier-detection (OD) performance of UniOD on 15 tabular datasets from ADBench when it is trained with varying numbers of historical datasets, denoted by M . Even with $M = 1$, UniOD already achieves competitive performance on the 'breastw' dataset. This early success is largely attributable to the structural resemblance between the single historical dataset and 'breastw' after both of them are converted into graphs. As M increases, UniOD is exposed to a more diverse set of graph-structured training examples, which enables the model to learn richer, structure-invariant representations of normal and anomalous patterns, thereby improving both its detection performance and its generalization ability to previously unseen datasets.

E.3 Results of Using Original Historical Datasets

In the training of UniOD, we use subsampling strategy on each historical dataset to create more data for training, which enhances the generalizaiton capability of UniOD. In this subsection, we

investigate how this influences the performance of UniOD by training UniOD using only the original historical datasets in Table 9.

Table 9: Average AUROC (%) and AUPRC (%) of UniOD on 15 tabular datasets of ADBench using only original historical datasets for training.

AUROC	Original	Subsampling
breastw	98.89	99.10
Cardiotocography	69.05	51.20
fault	51.28	69.60
InternetAds	61.62	63.50
landsat	47.11	69.10
optdigits	52.45	73.80
PageBlocks	89.94	88.20
pendigits	88.59	77.50
Pima	68.08	72.30
satellite	69.78	86.90
satimage-2	99.24	99.70
SpamBase	55.63	56.30
thyroid	95.08	94.10
Waveform	64.14	84.30
WDBC	98.54	98.40
AVG	73.96	78.93
AUPRC		
breastw	97.73	96.90
Cardiotocography	43.52	35.30
fault	35.17	49.10
InternetAds	30.00	32.80
landsat	20.21	28.10
optdigits	2.73	5.00
PageBlocks	43.68	46.20
pendigits	8.47	6.00
Pima	49.18	52.90
satellite	70.21	79.20
satimage-2	92.35	95.70
SpamBase	40.96	42.50
thyroid	29.17	44.30
Waveform	4.44	9.60
WDBC	52.35	57.80
AVG	41.34	45.43

E.4 Results of SVD+MLP

In this subsection, we replace the GIN and GT neural networks with MLPs to investigate the effectiveness of GIN and GT in UniOD. The experimental result is shown in Table 10. UniOD significantly outperforms SVD+MLP in most datasets, illustrating the effectiveness of using GIN and GT.

F Limitation and Future Work

In the experimental part, we mentioned that significant use of time arises from the graph-converting part which increases as data number grows. Also in this work, we primarily focus on tabular data, as data of other types can be converted into tabular data, we will conduct further studies on more data types and reducing the converting time doston in future work based on UniOD.

Table 10: Average AUROC (%) and AUPRC (%) of SVD+MLP on 15 tabular datasets of ADBench using only original historical datasets for training.

AUROC	SVD+MLP	UniOD
breastw	82.67	99.10
Cardiotocography	53.93	51.20
fault	51.42	69.60
InternetAds	52.09	63.50
landsat	54.88	69.10
optdigits	33.01	73.80
PageBlocks	65.39	88.20
pendigits	51.89	77.50
Pima	57.80	72.30
satellite	71.18	86.90
satimage-2	26.13	99.70
SpamBase	32.07	56.30
thyroid	86.79	94.10
Waveform	59.67	84.30
WDBC	36.05	98.40
AVG	54.33	78.93
AUPRC		
breastw	72.26	96.90
Cardiotocography	28.15	35.30
fault	39.20	49.10
InternetAds	27.11	32.80
landsat	22.02	28.10
optdigits	1.98	5.00
PageBlocks	18.56	46.20
pendigits	2.41	6.00
Pima	40.18	52.90
satellite	62.83	79.20
satimage-2	0.79	95.70
SpamBase	30.06	42.50
thyroid	44.88	44.30
Waveform	3.87	9.60
WDBC	2.77	57.80
AVG	26.47	45.43